A 3-D Study of Eddy Current Field and Temperature Rises in a Compact Bus Duct System

S. L. Ho[1], Y. Li[2], X. Lin[3], H. C. Wong[4], and K. W. E. Cheng[1]

[1]Department of Electrical Engineering, Hong Kong Polytechnic University, Kowloon, Hong Kong
[2]Research Institute of Special Electrical Machines, Shenyang University of Technology, Shenyang 110034, China
[3]Department of Electrical Engineering, Shenyang University of Technology, Shenyang 110034, China
[4]Industrial Center, the Hong Kong Polytechnic University, Kowloon, Hong Kong

In this paper, a three-dimensional eddy-current field model for calculating the eddy-current losses in a compact bus duct system is proposed. The temperature rises in the compact bus duct system, including both the long linear section and connecting unit, are evaluated using finite-element method when solving the governing thermal equations. The contact resistance between copper conductors and the corresponding temperature rises are measured in the test also. The computations are validated by test results and the results confirm the proposed algorithm is accurate and practical.

***Index Terms*—Bus duct system, eddy-current loss, temperature rise.**

I. Introduction

BUS DUCT systems (BDSs) instead of cables are commonly used in low voltage power distribution systems. They are installed in indoor power substations, tall buildings and factories [1]. Most BDS are air insulated with large size. Recently a new compact BDS, in which the space between two adjacent copper busbars is only 1 to 2 mm, is emerging in industry. The current carrying capacity of these compact BDS is generally larger than conventional ones and the enclosures of these BDS are made of aluminum alloy with excellent heat transfer characteristics. For BDS to be commercially viable, problems arising from induced magnetic heating and induced eddy-current in the enclosure as well as in the neutral (N) and protective earth (PE) busbars due to the heavy current that flows in modern BDS systems [1]–[3] must be addressed.

The most common design and computation method hitherto is to use lumped circuits together with empirical curves. Recently, the two-dimensional (2-D) finite-element method (FEM) has been used to calculate and analyze the magnetic field distribution in air insulated BDS [3]–[5], compact BDS [1], [2], [6] and single or 3-phase busbars without shielding [7], [8]. A 2-D hybrid FE-boundary-element formulation has also been applied in the magnetic field analysis of a four-conductor device with ac supply [7]. In some studies, the electromagnetic field is computed using FEM with the assumption that the exciting current is equal to the peak value of the steady-state ac current, however the eddy-current in the conductors is not taken into account in those studies [8]. In all the above-mentioned researches, only the long linear section of the BDS is modeled and analyzed. Nevertheless, an accurate BDS design requires a three-dimensional (3-D) study of the eddy-current field, induced magnetic heating and thermal behavior of the busbars. The analysis must also include both the linear section of BDS as well as the connecting units. A thorough investigation of the problem is thus of paramount importance in industry.

In this paper, a 3-D eddy-current field model to calculate the eddy-current losses is described. The temperature rises of copper busbars and enclosures in the compact BDS are determined by solving the thermal equations. A 2-kA compact BDS, including its long linear section and connecting unit, is studied and described. The measured contact resistance and temperature rise in the contact areas between copper conductors are incorporated in the computation. The results of computation and tests show good agreement.

II. Formulation

A. The 3-D Eddy Current Field Model

A typical compact BDS structure is shown in Fig. 1. To analyze the losses and to study the thermal problem in the compact BDS, the 3-D open boundary eddy-current field satisfying the following equations has to be evaluated first.

Using Maxwell's equation in which the magnetic vector potential and the electric scalar potential are introduced, the eddy-current field equations can be written as [9], [10]

$$\left.\begin{aligned}&\nabla\times\nu\nabla\times\dot{\mathbf{A}}-\nabla\nu\nabla\cdot\dot{\mathbf{A}}+\sigma\nabla\dot{\phi}+j\omega\sigma\dot{\mathbf{A}}=0\\&\nabla\cdot(-\sigma\nabla\dot{\phi}-j\omega\sigma\dot{\mathbf{A}})=0\end{aligned}\right\}\quad\text{in }\mathrm{V}_1 \tag{1}$$

$$\nabla\times\nu\nabla\times\dot{\mathbf{A}}-\nabla\nu\nabla\cdot\dot{\mathbf{A}}=\dot{\mathbf{J}}_s\quad\text{in }\mathrm{V}_2 \tag{2}$$

where V_2 is the area with source current, V_1 is the other area without source current, V is the whole solved area.

The boundary conditions are

$$\left.\begin{aligned}&\mathbf{n}\times\dot{\mathbf{A}}=0\\&\nu\nabla\cdot\dot{\mathbf{A}}=0\end{aligned}\right\}\quad\text{in }\mathrm{S}_1 \tag{3}$$

$$\left.\begin{aligned}&\nu\nabla\times\dot{\mathbf{A}}\times\mathbf{n}=0\\&\mathbf{n}\cdot\dot{\mathbf{A}}=0\end{aligned}\right\}\quad\text{in }\mathrm{S}_2 \tag{4}$$

$$\left.\begin{aligned}&\dot{\mathbf{A}}_1=\dot{\mathbf{A}}_2\\&\nu_1\nabla\cdot\dot{\mathbf{A}}_1=\nu_2\nabla\cdot\dot{\mathbf{A}}_2\\&\nu_1\nabla\times\dot{\mathbf{A}}_1\times\mathbf{n}_{12}=\nu_2\nabla\times\dot{\mathbf{A}}_2\times\mathbf{n}_{12}\\&\mathbf{n}\cdot(-j\omega\sigma\dot{\mathbf{A}}-\sigma\nabla\dot{\phi})=0\end{aligned}\right\}\quad\text{in }\mathrm{S}_{12}. \tag{5}$$

Digital Object Identifier 10.1109/TMAG.2006.871632

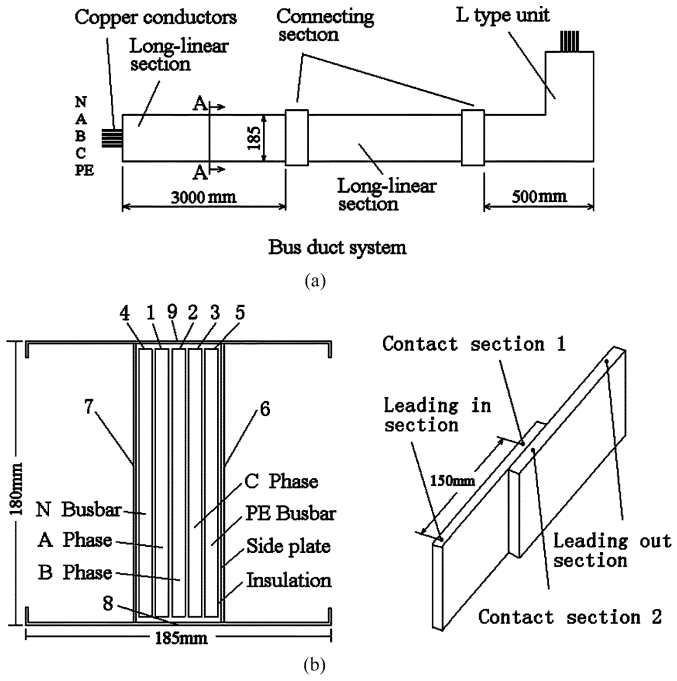

Fig. 1. The schematic structure of a compact BDS (a) The basic compact BDS, (b) Measurement points in the temperature rise test.

Introducing the boundary condition, the weighted residue equation can be written as

$$\int_V (\nu\nabla\times\mathbf{N}_i\cdot\nabla\times\dot{\mathbf{A}}+\nu\nabla\cdot\mathbf{N}_i\nabla\cdot\dot{\mathbf{A}}+j\omega\sigma\mathbf{N}_i\cdot\dot{\mathbf{A}} + \sigma\mathbf{N}_i\cdot\nabla\dot{\phi}-\mathbf{N}_i\cdot\dot{\mathbf{J}}_s)\,dv=0 \text{ in V} \quad (6)$$

$$\int_{V_1}\nabla N_i\cdot(j\omega\sigma\dot{\mathbf{A}}+\sigma\nabla\dot{\phi})\,dv=0 \quad \text{in } \mathrm{V_1} \quad (7)$$

where $\mathrm{N_i}$ is the weighted function. In this model the uniqueness condition can be satisfied and the boundary condition and the source current can be treated easily. By solving the equations, the magnetic flux, eddy-current and losses can be computed.

B. Thermal Equations

At steady-state, the thermal problem of the compact BDS satisfies the following thermal equilibrium equations:

$$P_K+P_M=Q_{\mathrm{KD}}+Q_{\mathrm{KF}} \quad (8)$$

where $\mathrm{P_M}$ and $\mathrm{P_K}$ are the power losses in Joule, respectively, in the phase busbars and the enclosure. $\mathrm{Q_{KD}}$ and $\mathrm{Q_{KF}}$ are, respectively, the heat loss from the enclosure to the surrounding air by radiation and convection.

Assuming the losses of the copper busbars and enclosures are dissipated as heat in a compact BDS, their corresponding temperature rises can be computed using FEM to solve the following thermal equations:

$$\begin{aligned}\Omega &: \nabla\cdot\lambda\nabla\theta=q_v\\ \Gamma_1 &: \theta=\theta_c\\ \Gamma_2 &: \lambda\frac{\partial\theta}{\partial n}=k_T(\theta_f-\theta)\end{aligned} \quad (9)$$

where Ω is the solved area, Γ is the boundary, λ is the coefficient of heat conductivity, $\mathrm{q_v}$ is the heat power per unit volume, the heat transfer coffieint $\mathrm{k_T}$ is determined experiementally to take into account of the heat transfer due to conduction, convection and radiation. θ is the temperature, θ_{f} is the ambient temperature.

In the computation, the ambient temperature is set to 19.8 °C which is the actual air temperature at the time of the test. The losses in the copper busbars and enclosures are taken as the source of heat power in a compact BDS. The heat transfer coefficient is an empirical parameter that incorporates the heat transfer relationship and the nature of the air flow pattern near the surface, the air properties and the geometry of the outside surfaces based on the nondimensional parameters that include the Grashof (Gr), Prandtl (Pr), Rayleigh (Ra) and Nusselt (Nu) numbers [1], [3]. With such assumptions, the heat transfer flux exchanged between the outside surfaces of the BDS and the surrounding air can then be quantified in the model as described below.

The Nusselt number can be represented by a power law

$$\mathrm{Nu}=C(\mathrm{Gr}\cdot\mathrm{Pr})^n. \quad (10)$$

The Grashof number is defined by the following:

$$\mathrm{Gr}=\left(\frac{g\beta\Delta\mathrm{T}\mathrm{L}^3}{v^2}\right) \quad (11)$$

where α is the gravitational acceleration, β is the coefficient of thermal expansion, $\Delta\mathrm{T}$ is the temperature difference, L is the equivalent linear dimension, v is the kinematic viscosity.

The Prandtl number is given by

$$\mathrm{Pr}=\frac{v}{\alpha} \quad (12)$$

where α is the thermal conductivity of the fluid (air in here), C and n in (10) are dimensionless constants dependent on the system, and for the case being studied n equals to 0.25. C is equal to 0.59 for the vertical surfaces, 0.54 for the upper horizontal surface and 0.27 for the lower horizontal surface [3].

Note that the Nusselt number is a nondimensional heat transmission coefficient defined by the following equation (applicable at steady-state) [1]:

$$\mathrm{Nu}=\frac{h_cL}{\alpha\theta} \quad (13)$$

where $\mathrm{h_c}$ gives a measure of the heat energy transferred per unit time and per unit area to the outside busbar surfaces. For the system being studied, the coefficient $\mathrm{h_c}$ (W/m^2 K) is 6.39 for the vertical surfaces, 5.32 for the upper horizontal surface and 2.66 for the bottom surface.

III. Calculations and Test of a 2-kA Compact BDS

A 2-kA compact BDS structure has been designed and built. Its eddy-current field, losses and temperatures are computed using the proposed algorithm. In the computation of the eddy-current field, the rated source current is 2 kA. The 3-phase source currents are assumed to be $-1.414+\mathrm{j}2.449$ kA in phase A, $2.828+\mathrm{j}0$ kA in phase B and $-1.414-\mathrm{j}2.449$ kA in phase C. Table I gives the losses of the busbar and enclosure in the scheme.

It is found from simulation that the eddy-current and losses are induced in the N-phase and PE-busbars as well as in the enclosures. The total losses of the compact BDS is 205.9 W/m. That includes 185.28 W/m in the A-, B-, and C-phase busbars and 20.6 W/m in the enclosure, N-phase and PE-busbars. It can

TABLE I
LOSSES IN THE BUSBARS AND ENCLOSURES IN A 2-kA COMPACT BDS (W/m)

N-phase busbar	A-phase busbar	B-phase busbar	C-phase busbar	PE-phase busbar	Enclosure
10.32	61.76	61.78	61.76	10.39	0.65

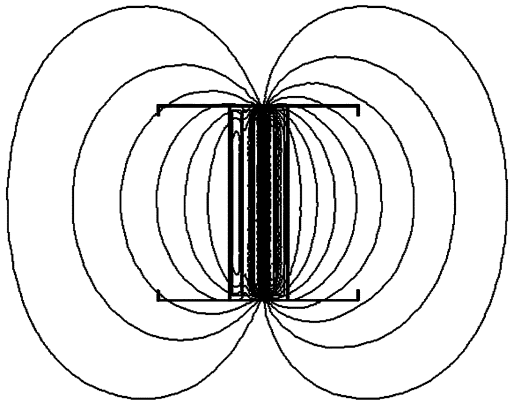

Fig. 2. The field on a cross section of the compact BDS.

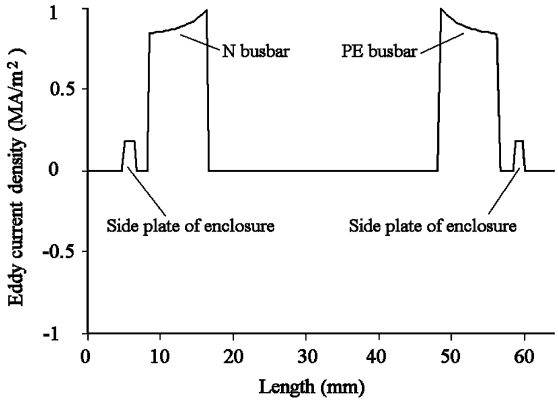

Fig. 3. Distribution of the eddy-current density in the compact BDS.

be seen that the eddy-current loss is about 10% of the total loss in the BDS. Because the resistivity of the copper busbars and the convective heat transfer coefficient are temperature dependent, their effects must be considered in the field and thermal calculations. Here, an initial temperature of copper conductors and the enclosure are assumed, an iterative method is used subsequently to calculate the losses and the thermal field.

Fig. 2 shows the field on a cross section of the compact BDS and Fig. 3 illustrates the distribution of the eddy-current density in the compact BDS. It can be seen that the maximum current in the N-/PE-busbars and in the side plate of the enclosure are, respectively, 0.98 MA/m^2 and 0.21 MA/m^2.

In order to check whether the compact BDS complies with the design, a test is carried out. In the test, the temperature of a horizontal busbar with the vertical copper conductors located at a distance of 200 mm from the ground is measured. The conductors are fed from one side with a low voltage 3-phase supply. The other sides of the busbars are short circuited. The N- and PE-phases are not connected. The temperature measurements are taken using thermocouples. Results of the test indicate that the temperature rises in the measured points on the busbar are in good agreement with the computed results. Table II gives the

TABLE II
TEST AND CALCULATED RESULTS OF TEMPERATURE RISE (K)

Positions	Tested	Calculated	Error (%)
1	38.8	37.3	-3.86
2	43.2	41.1	-4.86
3	39.5	37.2	-5.82
4	23.6	25.1	6.35
5	23.1	24.9	7.8
6	19.1	20.3	6.3
7	18.9	20.4	7.9
8	14.2	15.2	7.04
9	14.6	15.3	4.8

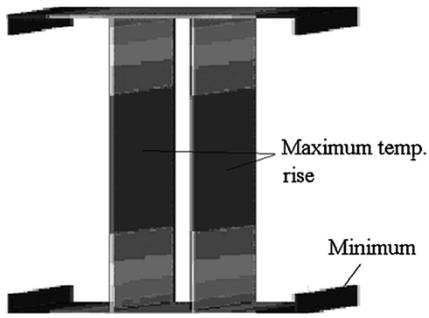

Fig. 4. The temperature rise of the enclosure.

TABLE III
MEASURED CONTACT RESISTANCE OF TWO CONDUCTORS ($\mu\Omega$)

	1	2	3	4	5	6	7	8	Average
A phase	1.7	2.2	1.4	2.1	2.3	0.9	1.8	2.7	1.89
B phase	2.2	1.6	1.8	2.3	3.0	2.1	2.3	1.9	2.15
C phase	2.8	2.6	2.0	2.8	2.3	1.8	1.9	2.7	2.24

test and computed temperature rise results [with the measurement positions as shown in Fig. 1(b)]. The maximum temperature rise limit of the hottest spot in the enclosure and busbar is 30 and 70 K, respectively.

Fig. 4 shows the distribution of the temperature rise in the enclosure of the compact BDS. It can be seen that the maximum temperature rise are at the two side plates of the enclosure.

Sections of busbars in BDS are usually bolted together electrically. The contact resistance of the connecting parts is one of the main factors influencing the thermal performance of BDS because contact resistance could have significant bearings upon the thermal characteristics of busbars. Indeed, the temperature rise at the contact is generally higher than that in other sections, such as the long linear sections, in most BDS. Obviously, the contact resistance is governed by factors such as the material characteristics, contact condition, contact pressing force and the degree of oxidization or state of sulfuration on the contact surfaces of the copper conductors. Thus accurate computation of the contact resistance is difficult. Therefore some tests are carried out to measure the contact resistance between two sections of the busbars as well as the temperature rises at the connecting sections of the BDS. Table III shows the contact resistances, which is the average of 8 measurements, in the 3-phase copper conductors. Table IV shows the temperature rise in the connecting sections of the BDS. It can be seen that there is very little difference between the temperature rises at the measuring positions in the same phase.

TABLE IV
MEASURED TEMPERATURE RISE IN THE CONNECTING SECTIONS (K)

	Leading in sections	Contact sections 1	Contact sections 2	Leading out sections
A phase	43.1	43.4	45.1	42.9
B phase	47.7	48.0	50.0	47.6
C phase	42.4	43.2	44.2	42.3

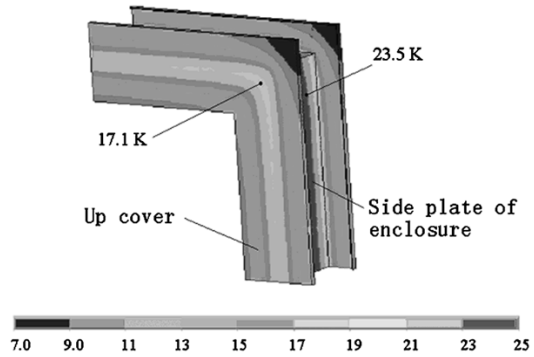

Fig. 5. Temperature rise of the L-type connecting unit.

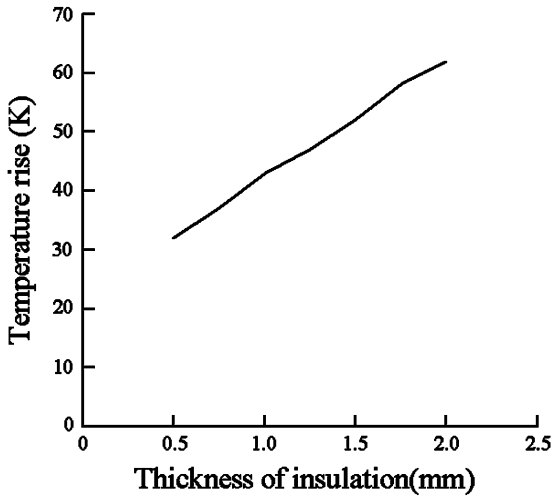

Fig. 6. Temperature rise of the copper conductor in the B-phase.

There are different types of connecting units in the BDS, such as the L-type unit, T-type unit and so on. Unlike normal long linear busbars, the temperature profile in the connecting units is 3-D in nature. Fig. 5 shows the temperature distribution in an L-type unit. Its temperature rise is 43.5 K in the B-phase copper conductor and is higher than the corresponding figures of 40.5 and 40.6 K, respectively, in the A- and C-phase copper conductors. The corresponding temperature rises in the neutral busbar, vertical enclosures and up cover are 25, 23.5, and 17.1 K, respectively.

The influence of the thickness of the insulation material upon the temperature rise of busbars have also been investigated. In the study the insulation thickness is changed from 0.5 to 2 mm whereas the current ratings and busbar sizes are assumed constant and the corresponding temperature rise of the copper conductor in the B-phase are shown in Fig. 6. It can be seen that the busbar temperature increases linearly with corresponding increases in the insulation material thickness. However the temperature rises in the enclosures are hardly affected. Upon careful consideration of the thermal and electric factors, the thickness of the insulation is chosen as 1 mm.

IV. CONCLUSION

Unlike other research results presented before, a 3-D eddy-current field method is described for calculating the eddy-current losses in a compact BDS in this paper. By solving the thermal equations, the temperature rises of the busbars as well as in the enclosure, the long linear section, the connecting section and the L-type connecting units in the BDS are all determined and analyzed. The calculated and tested results show good agreement.

REFERENCES

[1] A. Wu, "Finite element analysis of coupled magneto-thermal fields for compact busbar tranking system," *High Voltage Apparatus*, vol. 39, no. 4, pp. 7–10, 2003.
[2] C.-C. Hwang, "Analysis of electromagnetic and termal fields for a bus duct system," *Elect. Power Syst. Res.*, vol. 45, no. 1, pp. 39–45, 1998.
[3] H. Hedia, "Arrangement of phases and heating constraints in a busbar," *IEEE Trans. Magn.*, vol. 35, no. 3, pp. 1274–1277, May 1999.
[4] R. T. Coneybeer, "Steady-state and transient ampacity of bus bar," *IEEE Trans. Power Del.*, vol. 9, no. 4, pp. 1822–1829, Oct. 1994.
[5] S. W. Kim *et al.*, "Coupled finite element analytic technique for prediction of temperature rise in power apparatus," *IEEE Trans. Magn.*, vol. 38, no. 2, pp. 921–924, Mar. 2002.
[6] Y. Du, J. Burnett, and Z. C. Fu, "Experimental and numerical evaluation of busbar trunking impedance," *Elect. Power Syst. Res.*, vol. 55, no. 2, pp. 113–119, Aug. 2000.
[7] O. Bottauscio and E. Carpaneto, "Numerical and experimental evaluation of magnetic field generated by power busbar systems," in *Inst. Elect. Eng Proc. Gener. Trans. Distrib.*, vol. 143, Sep. 1996, pp. 455–460.
[8] D. G. Triantafyllidis, "Parametric short circuit force analysis of three phase busbar—A fully automated finite eelment approach," *IEEE Trans. Power Del.*, vol. 18, no. 2, pp. 531–536, Apr. 2003.
[9] O. Biro and K. Preis, "On the use of the magnetic vector potential in the finite element analysis of three dimensional eddy currents," *IEEE Trans. Magn.*, vol. 25, no. 4, pp. 3145–3159, Jul. 1989.
[10] D. Xie, "Vector potential and electrical scalar potential in 3D eddy current calculations," in *Proc. Electromagnetic Field in Electrical Engineering (BISEF'88)*, 1988, pp. 312–316.

Manuscript received June 26, 2005; revised November 20, 2005 (e-mail: eeslho@polyu.edu.hk).